Contract No.:

This manuscript has been authored by Battelle Savannah River Alliance (BSRA), LLC under Contract No. 89303321CEM000080 with the U.S. Department of Energy (DOE) Office of Environmental Management (EM).

Electro and electro-photo plasticity of CdZnTeSe and CdZnTe

Václav Dědič [1*], Jan Franc [1], Pavel Moravec [1], Roman Grill[1], Hassan Elhadidy [1], Vladimír Šíma [1], Miroslav Cieslar [1], Utpal N. Roy [2] and Ralph B. James [2]

[1] Charles University, Faculty of Mathematics and Physics, Ke Karlovu 5, CZ- 121 16, Prague 2, Czech Republic

[2] Savannah River National Laboratory, Savannah River Site, Aiken, SC 29808 USA

* Correspondence: dedicv@karlov.mff.cuni.cz; Tel.: +420 951552854

Abstract: We studied the influence of applied bias on of the Vickers microhardness HV 0.025 of CdZnTeSe and CdZnTe semi-insulating samples without and with the illumination of light at 870 nm. We observed that a small applied bias results in the hardening of the material. The effect is strongest at a bias of ±0.5 V and is further strengthened by additional illumination. We suggest that the observed positive electro and electro-photo plastic effects in CdZnTeSe and CdZnTe can be explained by an increase in the concentration of free electrons and holes injected from contacts in a biased sample or generated by illumination. These free carriers can be trapped at dislocations and induce a reconstruction of bonds at the dislocation core. The necessity to break the bonds before dislocation glide results in an increase of microhardness.

Keywords: electroplasticity, photoplasticity; CdZnTe; CdZnTeSe, spectral dependence

.

1. Introduction

Electro-plasticity is frequently observed as a decrease in the hardness of a material because of the flow of electric current. It is a common property of many metals and has found several applications in industrial processing and manufacturing [1-4]. It was observed for the first time from irradiation of a Zn crystal with electron beams [5]. Despite the clear success in applications, a theoretical explanation of the phenomenon is lacking [6]. The theoretical models include the hypothesis of action from a direct force on moving dislocations (electron wind) created by the electric current [7], an inertial dislocation depinning mechanism [8], magneto-plastic mechanism [9], and Joule heating [10]. The electric current densities at which the effect is observed in metals are typically very high (~10^3-10^4 A/cm^2).

In semiconductors, electro-plasticity was also observed in low-resistivity Ge and Si. In Ref. [11] Westbrook and Gillmann observed that the resistance of crystals to deformation by indentation lowers by 30% when a small bias (0.05-10 V) is applied parallel to the surface or perpendicular to the surface between the indenter and the material. In Ref. [12] the hardness of the near-surface region of ZnO was studied as a function of the surface charge. The observed dependence was explained by the transition of electrons between donor levels and unoccupied states in the conduction band, which enables dislocation motion. The hardness of materials can also be influenced by illumination [13, 14]. In CdTe a positive photo-plastic effect (hardening under illumination) was reported in Refs. [15, 16].

CdTe and $Cd_{1-x}Zn_xTe$ (x=0.1-0.2) found extensive applications in the generation of electric current in solar cells [17], medical applications for the detection of hard X-ray and gamma-ray radiation [18],

electro-optical modulators and other optical applications [19]. CdZnTeSe is currently under development as a future material in hard X-ray and gamma-ray detectors because the addition of Se was found to limit the formation of sub-grain boundaries and its networks, significantly reduce the Zn segregation, and improve the crystal's compositional homogeneity as compared to $Cd_{1-x}Zn_xTe$ [20].

The mechanical characteristics of the materials play an important role because both point defects and dislocations can be generated during material processing (thermal annealing, grinding, lapping, polishing, mounting, and other handling). These defects then can influence the performance of fabricated devices. Metal contacts are also used in most device structures. It is therefore important to understand how the optical and electric fields are able to influence the mechanical properties of CdTe-based compounds. We investigated the photo-plastic effect in CdZnTe and CdZnTeSe and its spectral dependence (see Ref. [21]). Hardening of the studied materials was observed upon illumination (positive photo-plastic effect). Materials used for radiation detectors must be semi-insulating to suppress the dark current. Research of their mechanical properties is of particular importance because the concentration of free carriers can change dramatically under bias and illumination and effects connected with trapping and recombination can be strong.

The purpose of the current investigation is to study the influence of an applied bias on the microhardness of CdZnTe and CdZnTeSe (electromechanical effect) and the combination of an applied bias with optical illumination (i.e., the influence of a combined electro-mechanical and photo effect).

2. Materials and Methods

We studied two semi-insulating samples – $Cd_{1-x}Zn_xTe$ (x~0.08-0.10, further denoted as CZT) and $Cd_{1-x}Zn_xTe_{1-y}Se_y$ (x ~ 0.08-0.10 and y ~ 0.04, further denoted as CZTS). Both crystals were prepared by the travelling heater method.

We measured the Vickers microhardness of the samples using a Qness Q10A automatic microhardness tester with a load of 25 grams (HV0.025) and an applied test force time of 10 s. Each data point representing the microhardness value is the result of averaging the values of ten indentations in one straight line shifted by 200 μm. The distance of the lines on which the other measured points were located was also approximately 200 μm. The selected distance is sufficient so that the measurements do not interfere with each other. We previously ensured that the samples showed a homogeneous dark microhardness distribution within the statistical error by measuring it at different positions.

The surface was polished with a final grit of 0.05 μm. We deposited thin Au layers on both large surfaces of the samples by thermal evaporation. The metal contacts were connected to a Keithley 2410 source meter. Then, we measured the dependence of the HV0.025 on the applied bias for voltages in the range of ±2 V.

To measure the electro-photo plastic effect during the microhardness measurements, we illuminated the top sample surface area below the indentation tip on the Au-grounded electrode layer using light from a bright light-emitting diode (LED) with a central wavelength at 870 nm and optical power of ~0.5 mW. The LED was placed approximately 15 mm from the sample at an angle of approximately 20° from the horizontal plane. The experimental setup is depicted in Figure 1. The LED has a divergent beam causing illumination of a larger area at the top electrode. The top gold electrode is thin and semi-transparent with almost constant spectral transmittance expected for the near-infrared range used in the experiments. The choice of the LED's central wavelength of 870 nm was motivated by a relatively strong photo-plastic effect for slightly below bandgap light recently observed for CZT and CZTS, while performing spectrally dependent measurements [21]. The use of a divergent beam of the LED was motivated by the generation of photocarriers over a larger volume of the biased sample.

We also measured the I-V characteristics of the samples with and without illumination using a Keithley 2410 source meter and Keithley 6514 electrometer by measuring the voltage on a 1 M∧ serial resistor. To determine the spectral absorption coefficients, we measured the spectral transmittance of the samples using a Fourier transform infrared spectrometer Bruker Vertex 80v equipped with a tungsten lamp, room temperature silicon photodiode detector, and CaF_2 beam splitter. All the measurements were carried out at the temperature of 303 K (~30°C).

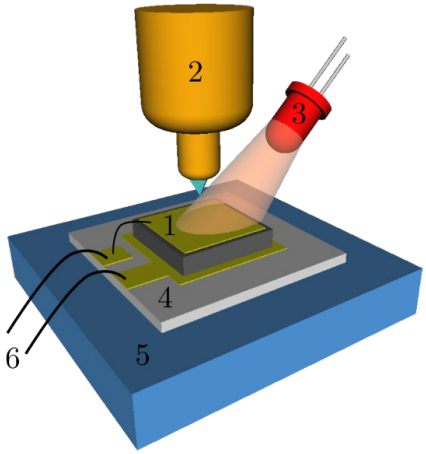

Figure 1. Experimental arrangement used in the microhardness experiments. 1-the measured sample with top gold electrode, which was grounded (i.e., the bottom electrode was biased). 2-Scheme of the Vickers diamond tip of the microhardness tester. 3-LED emitting at 870 nm. 4-Ceramic board equipped with gold contact areas. 5-base with a thermoelectric unit for temperature stabilization. 6-wires connected to the Keithley 2410 voltage source.

3. Results

In this section, we report the experimental results collected on the CZTS and CZT samples used in this study. The analysis of the data and a theoretical model are presented in Section 4.

Before the measurements of samples under voltage bias, we investigated the influence of Au layer on HV0.025 data. At first, we estimated its thickness. Based on the spectral transmission measurement and comparison with the ref.[22] we estimate the thickness of the gold layer to approximately 20 nm, which is negligible compared to the typical penetration depth of Vickers indenter in CZT and CZTS which is about 10 μm. On the basis of these facts, we expected that the gold layer will break immediately and will not have any effect. We have confirmed it by investigating the HV0.025 data on the same samples without Au contact and compared them with the results after Au contact deposition and zero bias. We found out that the HV0.025 remained indeed unchanged within statistical error. We thus conclude that the presence of a thin unbiased Au layer on the surface has no effect on the microhardness.

The results of the measurements of Vickers microhardness under bias without and with additional illumination at 870 nm are presented in Fig. 2 for the CZTS sample and in Fig. 3 for the CZT sample. The effects of biasing and optical excitation on HV0.025 are clearly visible in both samples.

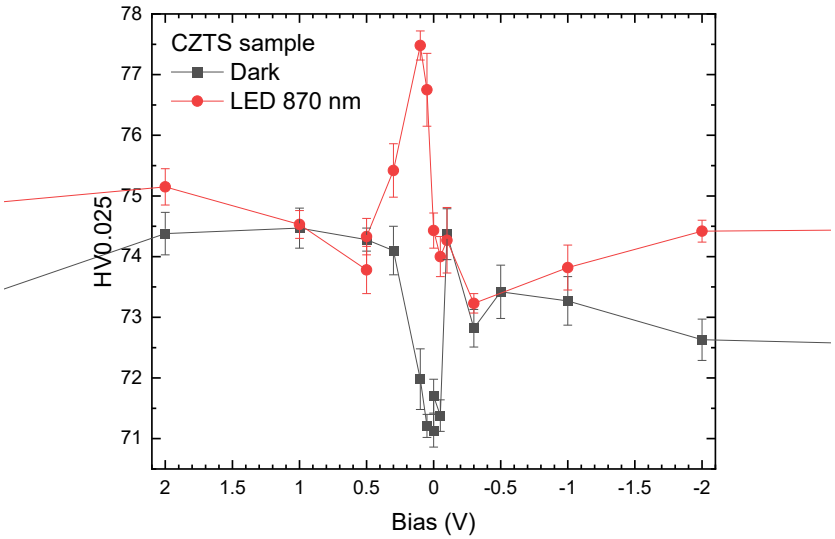

Figure 2. Evolution of the Vickers microhardness HV0.025 on the applied bias without and with illuminating light at 870 nm on the CZTS sample. The value of the voltage bias represents the potential at the indented surface.

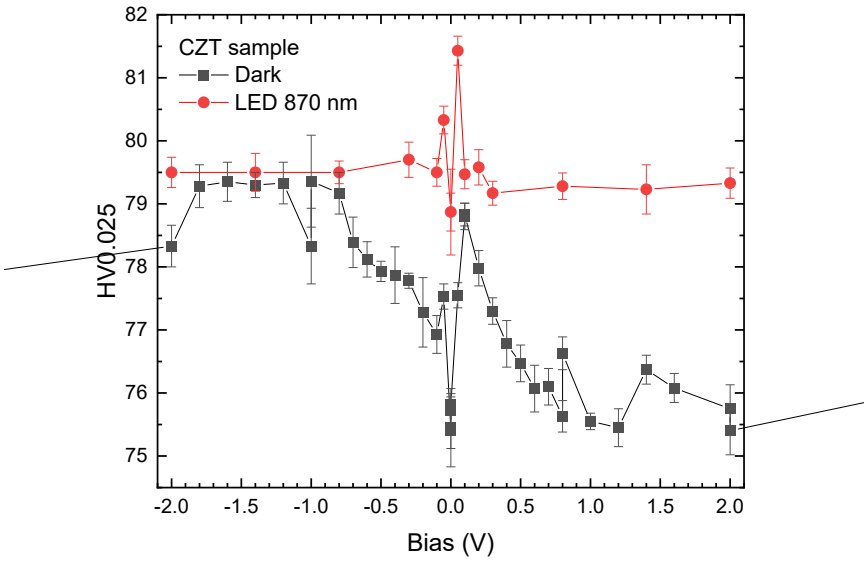

Figure 3. Evolution of the Vickers microhardness HV0.025 on the applied bias without and with illuminating light at 870 nm on the CZT sample. The value for the voltage bias represents the potential at the indented surface.

To better understand the electrical properties of the samples and the effects of LED optical excitation by near-band-gap light at 870 nm, we complemented the hardness measurements with measurements of the I-V characteristics in the dark and under illumination. We also investigated the shape of the absorption edge together with the spectral analysis of the LED.

Figures 4 and 5 show the current-voltage characteristics in the dark (black) and under 870-nm LED illumination (red) of CZTS and CZT samples, respectively. The low dark current of less than 1 nA at the chosen bias and the nearly linear measured I-V curves are consistent with the high resistivity of the

materials, low leakage current, and ohmic character of the contacts. The reason for the significantly different values of the photocurrent is discussed in Section 4.

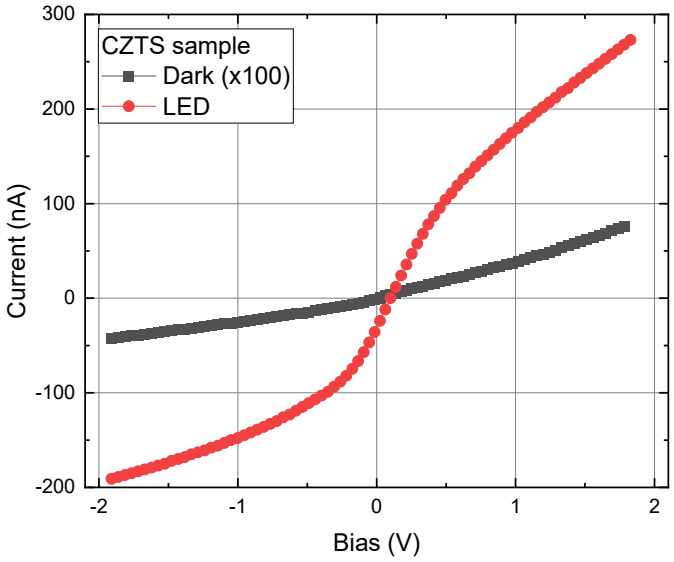

Figure 4. Current-voltage characteristics of the CZTS sample in the dark (black) and under illumination (red). The I-V curve in the dark is multiplied by 100 for better viewing of the data. The given bias represents the potential relative to the indented (illuminated) contact.

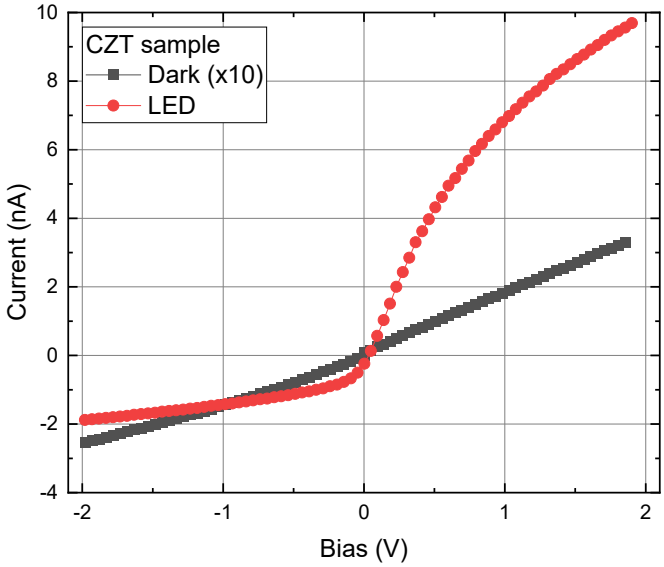

Figure 5. Current-voltage characteristics of the CZT sample in the dark (black) and under illumination (red). The I-V curve in the dark is multiplied by 10 for better viewing of the results. The value for the bias represents the potential relative to the indented (illuminated) contact.

Figure 6a plots the transmissivity of both the CZTS and CZT samples in the band-edge region and the spectral dependence of the 870 nm LED light used for excitation. The band-gap reduction in the CZTS sample relative to CZT is caused by the Se alloying. The measured transmittance was used for calculating the absorption coefficient according to the theory presented in [23]. The respective energy dependence of the absorption coefficient is shown in Fig. 6b, where the higher values of the absorption coefficient for higher photon energies, which are inaccessible by the transmission measurement for the optically thick sample, were obtained by extrapolation. It is seen that the LED energy dispersion covers a rather wide interval in the band-gap region, inducing simultaneously a strong excitation near the indented surface and a moderate excitation in the sample's bulk.

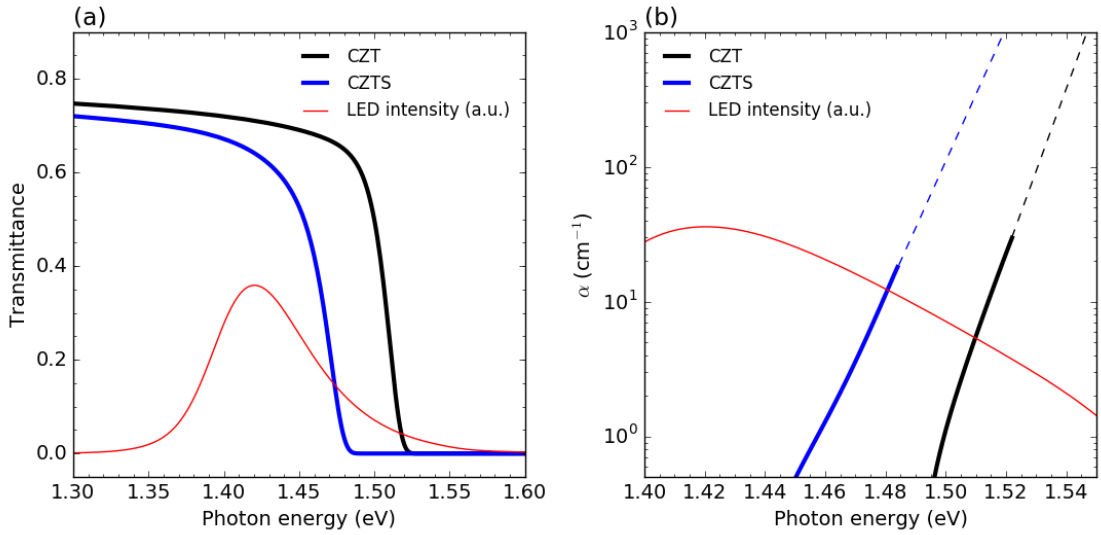

Figure 6: (a) Transmittance of the CZTS and CZT samples in the band-edge region and the spectral dependence of the 870-nm LED light used for sample excitation. (b) Absorption coefficient α of CZTS and CZT samples in the band-edge region together with the spectral dependence of 870-nm LED light used in the experiment. The dashed lines show the absorption coefficient acquired by extrapolation of low-energy data.

4. Discussion

Summarizing the experimental results of the measurements of bias- and light-induced changes of the Vickers microhardness HV0.025 in CZTS and CZT materials, we identified the following important features relevant to further data analysis and model definition. (i) The HV0.025 measured under illumination is greater to or similar to (i.e., within the statistical error) the HV0.025 in the dark for both samples. The photo-induced hardening of both materials is thus proven. (ii) The HV0.025 revealed fast changes at low bias between 0.3 V and 0 V. Similar findings were reported for the investigation of the electro-plasticity of Ge [11] and ZnO [12]. (iii) The HV0.025 in the dark vs. bias evolves nearly symmetrically in CZTS for both polarities whilst a significant difference between positive and negative bias appears for CZT. (iv) The symmetrical and nonsymmetrical character of the HV0.025 vs. bias in the dark correlates with the shape of the I-V photocurrent.

In addition to the experimental findings emerging from this investigation, we mention important information reported previously in the literature related to this study. An example is density functional theory calculations of electronic and atomic structures of glide partial dislocations in ZnS [24]. Authors revealed that carrier-dislocation interactions can induce more stable bond reconstructions at dislocation cores, which result in the hardening of the materials under illumination. Similar results may also be deduced from a prior first-principles study of dislocations in CdTe [25].

Based on the above findings and also considering the theoretical results, we propose a model of photo-plasticity. The principles of the model are as follows.

(a) The deformation forced by the indenter occurs through the movement of dislocations formed near the surface at the indentation spot (stacking fault). The indenter creates deformation stress that exceeds the critical shear stress, which activates the slip of dislocations.

(b) Based on the Frank-Reed model [26] of dislocation multiplication, the dislocation line is composed of segments with different deviations from crystal stoichiometry from purely cation-rich through ideal stoichiometric (screw) up to a completely anion-rich stoichiometry. The total stoichiometry deviation integrated along the whole dislocation line is close to zero. A schematic drawing of the dislocation loop propagation issued by a single stacking fault with outlined segments having different stoichiometry deviation is shown in Fig. 7. It is seen that the cation-rich and anion-rich regions accumulate at the opposite sides of the dislocation source, which could be rather distant regions on a microscopic scale. Thus, the charge transfer between the different-core dislocation regions considered in Ref. [25] could be rather slow to arrange an appropriate charge supply during deformation.

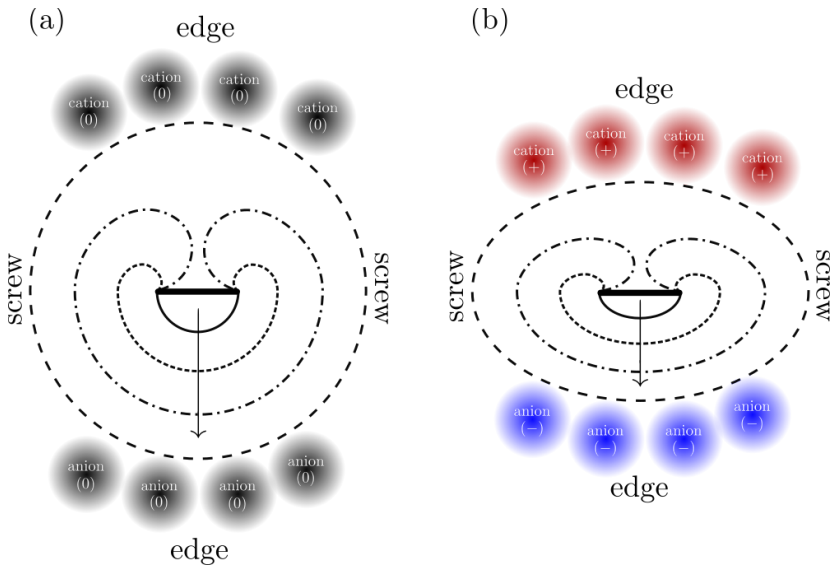

Figure 7: Schematic drawing of the propagation of dislocation loops issued by a single stacking fault with outlined segments with different stoichiometry deviations based on the Frank-Read model. The cation-rich and anion-rich regions accumulate at the opposite sides of the dislocation source. Uncharged dislocations outlined in the left panel (a) glide more easily than charged dislocations shown in the right panel (b).

(c) In unbiased semi-insulating semiconductors, such as the CZTS and CZT samples used in this study, there is very low density of free carriers available for capture by an extending dislocation line. Consequently, the dislocation remains mostly neutral. Considering the theoretical results in Ref. [24], neutral dislocations do not undergo reconstruction and remain in a configuration that is easy for glide, so that the hardness is low.

(d) Illuminating the sample leads to the generation of an excessive amount of free carriers that can be captured by dislocation segments according to their electrical character, resulting in dislocation reconstruction and ensuing hardening of the material.

(e) The plastic deformation is accompanied by the formation of various types of defects, dislocations, microcracks, and native point defects appearing as the result of the interaction of dislocations created in different active glide systems. These defects form new conducting channels in the crystal directly connected to the contact at the indented surface. The band structure of the sample with the deformation-induced impurity band is shown in Fig. 8(a).

(f) In the case of an applied bias, the deformation-induced defect states are filled by the charges from the adjacent contact, while the opposite charge is not supplied by the bulk (Fig. 8). One of the charge types (positive/negative) starts to dominate the other one. Subsequently, only appropriate

dislocation segments may pass the reconstruction. Due to this reason, the hardness stabilizes near the middle of the hardness at 0 V in the dark and for illumination.

(g) The hardening caused by dislocation charging due to the bias is amplified by the depth of the damage, which spreads much deeper than the depth penetrated by the indenter. The dislocation charging may be considered significant if corresponding states move under the bias in the potential exceeding $kT \approx 25$ meV. Such shift at the potential under pretty low bias 0.5 V yields the estimated depth of the damaged layer, i.e. the impurity band, reaches $\approx kT/eV_{bias}$ = 25/500*2 mm = 0.1 mm. Due to this reason, even a low bias of about 0.2 V suffices to charge the dislocations, especially at the head of the damaged region.

(h) The fact that the photo-plasticity shows a strong dependence on bias in illuminated CZTS where the larger photocurrent was measured (see Fig. 4) leads us to the conclusion that the indented region is distinguished by very high free-carrier recombination. Consequently, even the large influx of free carriers from the illuminated bulk does not compensate for the charge supplied by the contact.

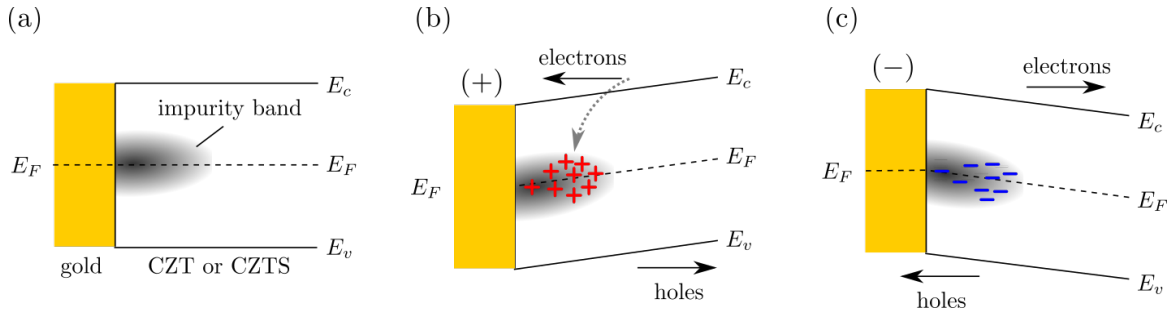

Figure 8: Band structure of the sample with a deformation-induced impurity band. Panels (a), (b), and (c) outline the charging at zero, positive and negative bias, respectively. The dotted arrow in panel (b) sketches the trapping of electrons neutralizing the positive charge formed by injected holes in the damaged region for the n-CZT considered in this investigation.

Items (a)-(h) consistently describe all the results measured for CZTS. In case of CZT, some discrepancies are noted. We expect that the reason is three-fold: (#1) The larger band gap of CZT lowers the absorption of the 870-nm LED spectrum, as documented in Fig. 6. (#2) The second difference lies in the predominantly n-type conductivity of CZT [27] in contrast to CZTS, where the electron and hole contributions to the conductivity are similar [28]. (#3) The third distinction may be due to the absence of Se alloying on the electrical properties and critical shear stress of dislocations.

Case #1 reflects the low effect of the illumination to the HV0.025 at zero bias, as seen in Fig. 3. The more complex behavior of HV0.025 vs. bias is apparent under dark conditions, which show a quasi-oscillatory character. We assume that the anomalous decrease of HV0.025 might be related to Case #2, where free electrons coming from the bulk are captured in the damaged region neutralizing or screening the positive charge supplied by the anode. Consequently, the charging of dislocations is suppressed, and HV0.025 approaches the value at zero bias. The less distinct suppression of HV0.025 at negative bias could be due to the specific defect structure of dislocations in CZT, where the negative charging of anion-core dislocation proceeds less distinctly than in the case of CZTS. Despite the unclear reason for the behavior of HV0.025 in CZT in the dark, the hardening induced by the illumination also remained valid for this sample.

5. Conclusion

We investigated the dependence of the Vickers microhardness of CdZnTe and CdZnTeSe samples on an applied bias and illumination by light at a wavelength of 870 nm. We observed that the microhardness HV0.025 in the dark vs. bias conditions evolves nearly symmetrically in CZTS for both polarities, whilst a significant difference between positive and negative bias appears in CZT. Results of measurements of microhardness with illumination confirm the presence of photo-induced hardening

for both materials. We present a qualitative model explaining the experimental data based on trapping of free electrons and holes on dislocation states. The trapped carriers induce a reconstruction of bonds at the dislocation core. The necessity to break the bonds before dislocation glide results in an increased microhardness. In summary, the HV is enhanced due to the charging of the neutral dislocation leading to a low HV. When either a positive or negative charge prevails, the HV increases. The hardening is strongest in the case of the illumination at zero bias when both free electrons and holes saturate the damaged region. Maximum HV is reached when both the cation- and anion-rich dislocation lines are charged. The change of microhardness induced by illumination is thus explained by the availability of free electrons and holes due to the generation of free carriers during specific illumination conditions. The hardening mediated by biasing is controlled by the supply of charge from the contact to the damaged region created by indentation.

Funding: This work was supported by the Grant Agency of the Czech Republic under the project. No. 19-17783S. Utpal Roy and Ralph B. James acknowledge the support of the U.S. Department of Energy, Office of Defense Nuclear Nonproliferation Research and Development, DNN R&D, and partial support by the SRNL Laboratory Directed Research and Development (LDRD) program.

Institutional Review Board Statement: "Not applicable"

Informed Consent Statement: "Not applicable"

Data Availability Statement: The data presented in this study are available on request from the corresponding author.

Acknowledgments: The authors greatly acknowledge Marta Čepová for her support with the measurements.

Conflicts of Interest: The authors declare no conflict of interest.

References

1. P. Bumgardner, B. P. Croom, N.N. Song, Y.Y. Zhang, X.D. Li. Low energy electroplasticity in aluminum alloys, Materials Science and Engineering A – Structural Material Properties Microstructure and Processing, 798 (2020) 140235. doi: 10.1016/j.msea.2020.140235.

2. L. Guan, G. Tang, P.K. Chu, Recent advances and challenges in electroplastic manufacturing processing of metals, Journal of Materials Research 25 (2010) 1215–1224, https://doi.org/10.1557/JMR.2010.0170

3. H. Xu, Y.J. Zou, Y. Huang, P.K. Ma, Z.P. Guo, Y. Zhou, Y.P. Wang, Enhanced Electroplasticity through Room-Temperature Dynamic Recrystallization in a Mg-3Al-1Sn-1Zn Alloy, Materials 14 (2021) 3739, doi: 10.3390/ma14133739.

4. K. Hariharan, M.J. Kim, S. T. Hong, D. Kim, J. H. Song, M. G. Lee, H.N. Han, Electroplastic behaviour in an aluminium alloy and dislocation density based modelling, Materials and Design 124 (2017) 131-142, doi: 10.1016/j.matdes.2017.03.072.

5. O. A. Troitskii and V. I. Likhtman, The effect of the anisotropy of electron and g radiation on the deformation of zinc single crystals in the brittle state, Dokl. Akad. Nauk. SSSR 148 (1963) 332–334.

6. N.K. Dimitrov, Y.C. Liu, M.F. Horstemeyer, A review of mechanisms in electro-mechanical coupling of ductile metals, Mechanics of Advanced Materials and Structures, 29:5 (2022) 705-716, doi: 10.1080/15376494.2020.1789925.

7. V. B. Fiks, Interaction of conduction electrons with single dislocations in metals, J. Exp. Theor. Phys. 53 (1982) 1209–1211.

8. A. V. Granato, Dislocation inertial model for the increased plasticity of the superconducting state, Phys. Rev. Lett. 27 (1971) 660–664, doi: 10.1103/PhysRevLett.27.660.

9. M. Molotskii, and V. Fleurov, Magnetic effects in electro-plasticity of metals, Phys. Rev. B. 52 (1995) 15829–15834, doi: 10.1103/PhysRevB.52.15829.

10. J. Magargee, F. Morestin, J. Cao, Characterization of ow stress for commercially pure titanium subjected to electrically assisted deformation, Journal of Engineering Materials and Technology 135 (2013) 041003

11. J. H. Westbrook and J. J. Gilman, An Electromechanical Effect in Semiconductors. J. Appl. Phys. 33 (1962) 2360-2369, doi: 10.1063/1.1728961.

12. J. S. Ahearn, J. J. Mills andA. R. C. Westwood, Effect of electrolyte pH and bias voltage on the hardness of the (0001) ZnO surface, J. Appl. Phys. 49 (1978) 96, doi: 10.1063/1.324341.

13. L. Carlsson, C. Svensson, Photoplastic Effect in ZnO, J. Appl. Phys. 41 (1970) 1652–1656. doi:10.1063/1.1659087.

14. S. Koubaiti, J.J. Couderc, C. Levade, G. Vanderschaeve, Vickers indentation on the (001) face of ZnS sphalerite under UV illumination and in darkness. Crack patterns and rosette microstructure. Acta Mater. 44 (1996) 3279–3291. doi:10.1016/1359-6454(95)00420-3.

15. T.J. Garosshen, J.M. Galligan, Photoplasticity and photonic control of dislocation densities in type II-VI semiconductors, J. Appl. Phys. 78 (1995) 5098–5102, doi:10.1063/1.359741.

16. L. Carlsson, C.N. Ahlquist, Photoplastic behavior of CdTe, J. Appl. Phys. 43 (1972) 2529–2536, doi:10.1063/1.1661555.

17. J.M. Burst, J.N. Duenow, D.S. Albin, E. Colegrove, M.O. Reese, J.A. Aguiar, C.-S. Jiang, M.K. Patel, M.M. Al-Jassim, D. Kuciauskas, CdTe solar cells with open-circuit voltage breaking the 1 V barrier, Nat. Energy 1 (2016) 1601. doi:10.1038/nenergy.2016.15.

18. T.E. Schlesinger, J.E. Toney, H. Yoon, E.Y. Lee, B.A. Brunett, L. Franks, R.B. James, Cadmium zinc telluride and its use as a nuclear radiation detector material, Materials Science And Engineering: R: Reports. 32 (2001) 103-189. https://doi.org/10.1016/S0927-796X(01)00027-4.

19. Y. Chang, C.H. Grein, J. Zhao, S. Sivanathan, C.Z. Wang,T. Aoki, D.J. Smith,P.S. Wijewarnasuriya,V. Nathan, Improved molecular beam epitaxy growth of HgCdTe on CdZnTe (211) B substrates using interfacial layers of HgTe/CdTe superlattices, J.Appl. Phys. 100 (2006), 114316.

20. U.N. Roy, G.S. Camarda, Y.Cui, R. Gul, A.Hossain, G. Yang, J. Zazvorka, V. Dedic, J.Franc, R.B. James, Role of selenium addition to CdZnTe matrix for room-temperature radiation detector applications, Scientific Reports 9 (2019) 1620.

21. J. Franc, V. Dědič, P. Moravec, M. Rejhon, R. Grill, H. Elhadidy, V. Šíma, M. Cieslar, M. Bratko, U. Roy and R. B. James, Spectral Dependence of the Photoplastic Effect in CdZnTe and CdZnTeSe, Materials 14(6) (2021) 1465. https://doi.org/10.3390/ma14061465

22. A. Axelevitch, B. Gorenstein and G. Golan, Investigation of Optical Transmission in Thin Metal Films. Physics Procedia, 32, (2012) 1–13. https://doi.org/10.1016/j.phpro.2012.03.510
23. P. Hlídek, J. Bok, J. Franc, R. Grill, Refractive index of CdTe: Spectral and temperature dependence, J. Appl. Phys. 90 (2001) 1672.

24. K. Matsunaga, S. Hoshina, M. Ukita, Y. Oshima, T. Yokoi, A. Nakumara, Carrier-trapping induced reconstruction of partial-247 dislocation cores responsible for light-illumination controlled plasticity in an inorganic semiconductor, Acta Mater. 195 (2020) 645-653. https://doi.org/10.1016/j.actamat.2020.06.010

25. K. E. Kweon, D. Aberg, V. Lordi. First-principles study of atomic and electronic structures of 60◦ perfect and 30/90 partial glide dislocations in CdTe. Phys. Rev. B 93 (2016) 174109. https://doi.org/10.1103/PhysRevB.93.174109

26. F.C. Frank, W.T. Read, Jr., Multiplication processes for slow moving dislocations, Phys. Rev. 79 (1950) 722.

27. A. Musiienko, R. Grill, P. Hlídek, P. Moravec, E. Belas, J. Zázvorka, G. Korcsmáros, J. Franc and I. Vasylchenko, Deep levels in high resistive CdTe and CdZnTe explored by photo-Hall effect and photoluminescence spectroscopy. Semicond. Sci. Technol. 32 (2017) 015002.

28. J. Pipek, M. Betušiak, E. Belas, R. Grill, P. Praus, A. Musiienko, J. Pekárek, U.N. Roy, and R.B. James, Charge Transport and Space-Charge Formation in Cd1−xZnxTe1−ySey Radiation Detectors, Phys. Rev. Applied 15 (2021) 054058.